

**NASA TECHNICAL
MEMORANDUM**

NASA TM X- 72805

NASA TM X- 72805

(NASA-TM-X-72805) TRACTION CHARACTERISTICS
OF A 30 BY 11.5-14.5, TYPE 8, AIRCRAFT TIRE
ON DRY, WET AND FLOODED SURFACES (NASA)
28 p HC \$4.00

CSCL 01C

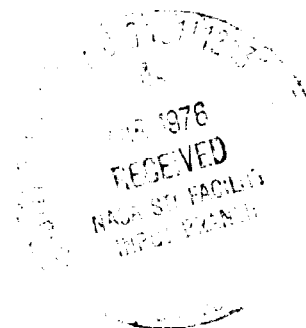
N76-18496

G3/37 Unclass
18419

TRACTION CHARACTERISTICS OF A 30 x 11.5-14.5, TYPE VIII,
AIRCRAFT TIRE ON DRY, WET AND FLOODED SURFACES

By

Thomas J. Yager and Robert C. Dreher
Langley Research Center



This informal documentation medium is used to provide accelerated or special release of technical information to selected users. The contents may not meet NASA formal editing and publication standards, may be revised, or may be incorporated in another publication.

**NATIONAL AERONAUTICS AND SPACE ADMINISTRATION
LANGLEY RESEARCH CENTER, HAMPTON, VIRGINIA 23665**

1. Report No. TM X- 72805		2. Government Accession No.		3. Recipient's Catalog No.	
4. Title and Subtitle TRACTION CHARACTERISTICS OF A 30 x 11.5-14.5, TYPE VIII, AIRCRAFT TIRE ON DRY, WET AND FLOODED SURFACES				5. Report Date February 1976	
				6. Performing Organization Code	
7. Author(s) Thomas J. Yager and Robert C. Dreher				8. Performing Organization Report No.	
				10. Work Unit No. 505-08-31-01	
9. Performing Organization Name and Address NASA Langley Research Center Hampton, Virginia 23665				11. Contract or Grant No.	
				13. Type of Report and Period Covered Technical Memorandum	
12. Sponsoring Agency Name and Address National Aeronautics & Space Administration Washington, D. C. 20546				14. Sponsoring Agency Code	
15. Supplementary Notes					
16. Abstract <p>A limited test program was conducted at the Langley aircraft landing loads and traction facility to extend and supplement the braking and cornering data determined from an earlier investigation on a 30 x 11.5-14.5, type VIII, aircraft tire. The primary purpose of this investigation was to obtain information necessary to refine the tire/runway friction model for use in the development of an aircraft ground performance simulation. The tire traction data, which included the drag-force and cornering-force friction coefficients, were obtained on dry, wet and flooded runway surfaces at ground speeds ranging from 5 to 100 knots and at yaw angles extending up to 12°. These friction coefficients are presented as a function of slip ratio to satisfy the needs of the simulation. In addition, selected friction characteristics, namely, the maximum and skidding drag coefficients and the maximum cornering coefficient are presented as a function of both ground speed and yaw angle to extend existing data on that tire size. The results of this investigation substantiated the findings from similar tests previously conducted on this tire in which the tire braking and cornering capabilities were shown to be affected by vehicle ground speed, wheel yaw attitude and the extent of surface wetness.</p>					
17. Key Words (as requested by Author(s)) Aircraft tire Braking traction Cornering traction Runway wetness Friction characteristics			18. Distribution Statement Unclassified - Unlimited		
19. Security Classif. (of this report) Unclassified	20. Security Classif. (of this page) Unclassified	21. No. of Pages 26	22. Price \$3.75		

TRACTION CHARACTERISTICS OF A 30 x 11.5-14.5, TYPE VIII, AIRCRAFT TIRE ON DRY, WET AND FLOODED SURFACES

By Thomas J. Yager and Robert C. Dreher
Langley Research Center

SUMMARY

A limited test program was conducted at the Langley aircraft landing loads and traction facility to extend and supplement the braking and cornering data determined from an earlier investigation on a 30 x 11.5-14.5, type VIII, aircraft tire. The primary purpose of this investigation was to obtain information necessary to refine the tire/runway friction model for use in the development of an aircraft ground performance simulation. The tire traction data, which included the drag-force and cornering-force friction coefficients, were obtained on dry, wet and flooded runway surfaces at ground speeds ranging from 5 to 100 knots and at yaw angles extending up to 12° . These friction coefficients are presented as a function of slip ratio to satisfy the needs of the simulation. In addition, selected friction characteristics, namely, the maximum and skidding drag coefficients and the maximum cornering coefficient are presented as a function of both ground speed and yaw angle to extend existing data on that tire size. The results of this investigation substantiated the findings from similar tests previously conducted on this tire in which the tire braking and cornering capabilities were shown to be affected by vehicle ground speed, wheel yaw attitude and the extent of surface wetness.

INTRODUCTION

This paper presents the results of a limited investigation conducted at the Langley aircraft landing loads and traction facility to supplement data obtained earlier (ref. 1) on the traction capability of a main gear tire used on a high performance jet fighter aircraft. The primary purpose of this investigation was to obtain information necessary to refine the tire/runway friction model for use in the development of an aircraft ground performance simulation. In particular, interest was centered on determining the traction characteristics of a 3-groove, 30 x 11.5-14.5, type VIII, aircraft tire on dry, wet and flooded surfaces. Tire braking and cornering characteristics, which included the drag-force and cornering-force friction coefficients, were obtained during brake cycles from free-rolling to locked-wheel conditions, over a range of yaw angles from 0° to 12° and at ground speeds from 5 to 100 knots. These characteristics are presented in a form which is compatible with the computer input requirements in the aircraft ground simulation program.

SYMBOLS

Values are given in both SI and U.S. Customary Units. The measurements and calculations were made in U.S. Customary Units. Factors relating the two systems are presented in reference 2.

μ_d	drag-force friction coefficient, parallel to direction of motion, $\frac{\text{Drag force}}{\text{Vertical force}}$
$\mu_{d,\max}$	maximum drag-force friction coefficient
$\mu_{d,\text{skid}}$	skidding drag-force friction coefficient
μ_s	cornering-force friction coefficient, perpendicular to direction of motion, $\frac{\text{Side force}}{\text{Vertical force}}$
$\mu_{s,\max}$	maximum cornering-force friction coefficient

APPARATUS AND TEST PROCEDURE

Tires

The test tires for this investigation were 3-groove, 30 x 11.5-14.5, 24-ply-rating, type VIII, aircraft tires similar to those used on a current jet fighter aircraft. Two such tires were employed during the test sequence as the initial tire was replaced when the tread wear reached 50 percent. A photograph of one test tire is shown in figure 1 together with tire footprints obtained at the extremes in vertical load to illustrate loading effects on the contact area. The vertical load on the tires was varied with ground speed as shown in figure 2 to simulate the effects of wing lift. This loading was determined from aircraft tests and ranged from approximately 55.6 kN (12 500 lb) at 100 knots to 69 kN (15 500 lb) at 5 knots. The inflation pressure of the tires throughout the test program was maintained at 1827 kPa (265 psi).

Test Surfaces

Tire braking and cornering data were obtained at the landing loads track over a 183 m (600 ft) section of the concrete test runway divided into three approximately equal segments. The surface of one segment was maintained dry, one was wetted with water to a depth which ranged between 0.05 and 0.08 cm (0.02 and 0.03 in.), and the third was flooded to a water depth which extended from 0.5 to 0.8 cm (0.2 to 0.3 in.). Photographs of

the three segments ready for test are presented in figure 3. Because this test surface has been used extensively over the past three years and has undergone several rubber removal programs, its surface texture is no longer consistent. Texture measurements using the grease sample technique (see ref. 3) resulted in the following average texture-depth values: 91 μm (0.0036 in.) for the dry concrete, 115 μm (0.0045 in.) for the wet surface, and 144 μm (0.0057 in.) for the flooded test section. It should be noted that the wet and flooded runway sections of this investigation are the same corresponding sections used in the earlier rain tire program (ref. 1) but there has been a reduction in the average texture depth of these two test surfaces during the 13-month interim.

A factor which significantly effected the dry braking data was the accumulation of rubber on the test surface, which would occur during locked-wheel braking and all operations at high tire yaw angles. This rubber build-up tended to reduce the texture of the surface and therefore the braking traction capability. Although the surface was cleaned of rubber deposits about midway through the program and attempts were made to vary the location of the dry cycle on the runway, some overlapping did occur and hence much of the dry braking data were obtained on a surface made smooth by rubber deposits rather than a clean, textured, concrete surface.

Test Facility

The investigation was conducted at the Langley aircraft landing loads and traction facility, described in references 4 and 5, and utilized the main test carriage pictured in figure 4. The aircraft test tire, wheel and brake assembly were mounted on an instrumented dynamometer which measured the various axle loadings. Figure 5 presents a schematic of the dynamometer instrumentation which consisted of load beams to measure vertical, drag and lateral forces and links to measure brake torque, all at the wheel axle. Additional instrumentation was provided to measure brake pressure, wheel angular velocity, and carriage horizontal displacement and velocity. Continuous time histories of the output of the instrumentation during a run were obtained by tape recorders mounted on the test carriage.

Test Procedure

The procedure followed for most test runs involved propelling the carriage to the desired ground speed, releasing the drop test fixture to apply the preselected vertical load on the tire, and subjecting the tire to controlled brake cycles on the dry surface first and subsequently on the wet and flooded surfaces. A brake cycle consisted of actuating the brake-pressure solenoid valve at predetermined locations along the track, thus braking the tire from a free-rolling condition to a locked-wheel skid, and then releasing the brake pressure to allow tire spinup prior to the next cycle. Nominal carriage speeds for these tests consisted of 5 knots, obtained by towing the carriage with a ground vehicle, and 50, 75 and 100 knots, obtained by propelling the carriage with the hydraulic water jet.

Evaluation of combined tire braking and cornering traction was achieved by rotating and locking in place prior to each run the entire test fixture dynamometer to yaw angles of 0° to 12° in 3° increments. The instrumentation measurements, recorded on tape, provided a complete time history of the test tire behavior during the course of a run.

RESULTS AND DISCUSSION

General

Figure 6 presents typical time histories of the significant parameters recorded during a single brake cycle. These parameters include the carriage speed, test wheel tangential velocity, the tire-to-ground forces in the drag, vertical and side directions, and the brake pressure and resulting torque. Also presented are time histories of the drag-force friction coefficient μ_d parallel to the direction of motion and the cornering-force friction coefficient μ_s perpendicular to the direction of motion - both computed from the measured force data. The wheel slip ratio (ratio of relative slip velocity between the wheel and the surface to the carriage velocity) was computed from the test wheel and carriage velocity measurements and is included as a function of time in the figure.

The drag-and side-force friction coefficients computed during each brake cycle were replotted as a function of wheel slip ratio to be compatible with the input requirements in the aircraft ground simulation program. Figure 7 is a typical example of these computer plots and serves to illustrate how the data were faired for analysis and application. For each test condition the faired curves representing the time history data obtained during a brake cycle were used to determine: (a) the variation of both drag-force and cornering-force friction coefficient with wheel slip ratio; (b) the maximum drag-force friction coefficient $\mu_{d,max}$ encountered during wheel spin-down; and (c) the skidding drag-force friction coefficient $\mu_{d,skid}$ measured during wheel lockup. Maximum values of cornering force friction coefficient $\mu_{s,max}$ were also determined for each test condition from fairings of the data before braking was initiated. The following sections discuss the variation of μ_d and μ_s with slip ratio on dry, wet and flooded surfaces (figures 8, 9 and 10) and the variation of $\mu_{d,max}$, $\mu_{d,skid}$ and $\mu_{s,max}$ with ground speed (figure 11) and yaw angle (figure 12). It should be pointed out that the values for $\mu_{d,skid}$ and $\mu_{s,max}$ in figures 11 and 12 were determined from fairings of relatively long duration both before braking, to obtain $\mu_{s,max}$, and after the wheel had locked up, to obtain $\mu_{d,skid}$. Since the corresponding values of μ_s and μ_d in figures 8, 9 and 10 were essentially instantaneous values, some differences in the magnitudes of these coefficients do exist between the two sets of data.

Variation of Friction Characteristics with Slip Ratio

The data presented in figures 8, 9, and 10 summarize the variation in tire traction with slip ratio on a dry, wet and flooded surface, respectively, at ground speeds of 50, 75 and 100 knots and at each test yaw angle. The curves of these figures are based on fairings of computer plots similar to that shown in figure 7 and represent fractions of a second in real time as illustrated by the brake cycle time histories of figure 6 where it required approximately one-tenth of a second for the wheel to completely spin down. The data which describes the dry tire traction, as presented in figure 8, are limited to yaw angles of 0- and 12-degrees because data from tests at other yaw angles on that surface were compromised by the presence of rubber deposits. Figure 8 exhibits the classical variation in drag-force friction coefficient with slip ratio on a dry surface in that μ_d increases with brake application from the free-rolling value, reaches a maximum, and then decreases to lower levels as the wheel approaches lockup. The figures show that μ_d peaks at a slip ratio of about 0.15 at all three speeds for the unyawed tire and is a maximum at a slip ratio between 0.3 and 0.4 when the tire is yawed to 12°. As shown in figure 8(a), wheel lockup did not occur during the 50-knot run with the unyawed tire due to an inadvertent early release of brake pressure.

No side-force friction coefficient μ_s is developed with an unyawed tire, of course. However, the figure shows that at the 12° yaw angle, μ_s is at a maximum during free roll, then decreases rapidly with brake application to near zero at or before the wheel locks up.

The variation of drag-and side-force friction coefficients developed by the tire while undergoing braking at each of the test yaw angles is shown in figure 9 for the wet surface and figure 10 for the flooded surface. The variation of both μ_d and μ_s is similar to that observed on the dry surface; however, as might be expected, the magnitude of these friction coefficients is considerably reduced and the peak μ_d not nearly as well defined. Tire braking data on the wet and flooded surfaces indicate that μ_d levels decrease as yaw angle is increased, and that the variation of μ_s is nearly independent of yaw angle. On both the wet and the flooded surfaces, the μ_s curves indicate that tire steering capability is completely lost at or before reaching a slip ratio of 0.8.

Variation of Friction Characteristics with Ground Speed

The effect of ground speed on certain tire braking and cornering characteristics developed during operations on dry, wet and flooded surfaces is shown in figure 11 for each of the five different test yaw angles. Data obtained on areas of the dry surface test section which contained rubber deposits from previous braking cycles are identified. The effect of the rubber contamination is to greatly reduce the tire traction during braking. For example, during brake cycles made with the tire yawed 6° and at a speed of 5 knots, the maximum drag-force friction coefficient was reduced from 0.5 on the clean surface to 0.3 on the same surface coated with rubber.

Maximum drag-force friction coefficient.- The data of figure 11 indicate that the maximum drag-force friction coefficient $\mu_{d,max}$ decreases with increasing ground speed over the range of yaw angles investigated. This decrease was observed for all runway surface conditions although it is much less pronounced on the dry than on the two wetted surfaces, which corroborates trends observed in references 6 to 10.

Little difference appears to exist in the magnitude of $\mu_{d,max}$ as developed on the wet and flooded test surfaces for similar speeds and yaw angles, despite a significant difference in water depth and associated dynamic hydroplaning effects. Two factors may contribute to the high $\mu_{d,max}$ level on the flooded surface. First, the texture depth of the flooded surface is approximately 25-percent higher than that of the wet surface which should contribute to the traction at speeds at least up to 100 knots, since that speed is well below the computed dynamic hydroplaning speed of 147 knots for the test tire. Second, the flooded surface, by virtue of its greater water depth, induces higher fluid drag than the wet surface. It should be pointed out that the data obtained from the flooded surface agrees closely with that obtained during the rain tire program and reported in reference 1.

Skidding drag-force friction coefficient.- The skidding drag-force friction coefficient $\mu_{d,skid}$ is shown in figure 11 to decrease with increasing ground speed in a manner similar to $\mu_{d,max}$ but at somewhat lower friction levels. This trend is noted at all test yaw angles and on the dry, wet and flooded surfaces. Values of $\mu_{d,skid}$ on the flooded surface are shown to be equal to or slightly higher than those on the wet surface, particularly at the higher ground speeds. This variation apparently results from the same reasons identified in the preceding section.

Maximum cornering-force friction coefficient.- The data in figure 11 indicate that on a dry surface the maximum cornering-force friction coefficient $\mu_{s,max}$ increases with increasing ground speeds for yaw angles up to about 9° - the rate of increase becoming less pronounced as the yaw angle is increased - and decreases slightly with speed at 12° yaw. Values of $\mu_{s,max}$ on the wet and flooded surfaces are quite similar for all yaw angles and tend to decrease with increasing ground speed.

Variation of Friction Characteristics with Yaw Angle

The data of figure 11 were replotted in figure 12 to show more clearly the effect of changing yaw angle on the drag-force and cornering-force friction coefficients as developed by the test tires at various ground speeds and surface wetness conditions.

Maximum drag-force friction coefficient.- As shown in figure 12, the highest values of $\mu_{d,max}$ were developed at the lowest test ground speed with the tire in the unyawed attitude. In general, the magnitude of $\mu_{d,max}$ decreased with increasing yaw angle over the range of yaw angles and test speeds investigated, although the extent of the decrease appears to be much

less pronounced at the higher test speeds. Note that at the five-knot test speed, $\mu_{d,max}$ at all yaw angles is essentially independent of the wetness condition, since at that speed, the effects of hydroplaning on the wetted surfaces are nil. It is of further interest to observe that the effect of contaminating the surface with rubber is to reduce the available friction even at five knots.

Skidding drag-force friction coefficient.- Yaw angle appears to have very little effect on $\mu_{d,skid}$. The data in figure 12 show that values of $\mu_{d,skid}$ remain very nearly constant throughout the range of yaw angles tested, although a certain dependence on ground speed is shown. The values of $\mu_{d,skid}$ on the wet and flooded surfaces are about equal but slightly less than those developed on the dry surface because of the thin film lubrication provided by the presence of water. Again the fluid drag plus better surface texture make the flooded data somewhat higher than the respective wet data.

Maximum cornering-force friction coefficient.- At five knots, the maximum cornering-force friction coefficient, $\mu_{s,max}$ increases with increasing yaw angle up to and including the maximum test angle on all test surfaces. At the higher speeds, $\mu_{s,max}$ increases with an increase in yaw angle, reaches a maximum value, and then decreases with further increases in yaw angle. Peak values appear to occur between 6° and 9° on the dry surface and between 3° and 6° on the wet and flooded surfaces. The variation of $\mu_{s,max}$ with yaw angle on the dry surface appears to be independent of speed at least in the range of 50 to 100 knots; however, on the wet and flooded surfaces, the variation with yaw angle is dependent upon speed and is approximately the same on both the wet and the flooded surfaces.

CONCLUDING REMARKS

A limited investigation was conducted at the Langley aircraft landing loads and traction facility to extend and supplement the braking and cornering traction data acquired in an earlier program with the 30 x 11.5-14.5, type VIII, aircraft tire. The primary purpose of this investigation was to obtain information necessary to refine the tire/runway friction model for use in the development of an aircraft ground performance simulation. The investigation entailed braking tests from free roll to locked wheel skids on dry, wet and flooded runway surfaces over a range of yaw angles from 0° to 12° and at ground speeds from 5 to 100 knots.

The results from these tests substantiated the findings from similar tests previously conducted on this tire in which the tire braking and cornering capabilities were shown to be affected by vehicle ground speed, wheel yaw attitude and the extent of surface wetness. The overall braking traction was found to decrease with increases in both speed and surface water depth; further, the maximum available braking coefficient decreased with increased yaw angle while the somewhat lower skidding coefficient appeared to be insensitive to yaw angle changes. The tire steering or cornering traction was a maximum when the wheel was freely rolling and decreased rapidly

with braking, reaching zero at or before wheel lockup. Wetting the surface or increasing the ground speed generally tended to decrease the tire cornering capability. The yaw angle at which the maximum cornering coefficient was developed typically decreased with increased speed and with surface wetness. The presence of rubber deposits on the dry test surface resulted in significant reductions in tire traction.

REFERENCES

1. Dreher, Robert C.; and Tanner, John A.: Experimental Investigation of the Braking and Cornering Characteristics of 30 x 11.5-14.5, Type VIII, Aircraft Tires with Different Tread Patterns. NASA TN D-7743, 1974.
2. Anon.: Metric Practice Guide. E 380-72, Amer. So. Testing & Mater., June 1972.
3. Leland, Trafford J. W.; Yager, Thomas J.; and Joyner, Upshur T.: Effects of Pavement Texture on Wet-Runway Braking Performance. NASA TN D-4323, 1968.
4. Joyner, Upshur T.; Horne, Walter B.; and Leland, Trafford J. W.: Investigations on the Ground Performance of Aircraft Relating to Wet Runway Braking and Slush Drag. AGARD Rept. 429, January 1963.
5. Joyner, Upshur T.; and Horne, Walter B.: Considerations on a Large Hydraulic Jet Catapult. NACA TN 3203, 1954.
6. Horne, Walter B.; and Leland, Trafford J. W.: Influence of Tire Tread Pattern and Runway Surface Condition on Braking Friction and Rolling Resistance of a Modern Aircraft Tire. NASA TN D-1376, 1962.
7. Horne, Walter B.; and Dreher, Robert C.: Phenomena of Pneumatic Tire Hydroplaning. NASA TN D-2056, 1963.
8. Horne, Walter B.; Yager, Thomas J.; and Taylor, Glenn R.: Review of Causes and Alleviation of Low Tire Traction on Wet Runways. NASA TN D-4406, 1968.
9. Byrdsong, Thomas A.: Investigation of the Effect of Wheel Braking on Side-Force Capability of a Pneumatic Tire. NASA TN D-4602, 1968.
10. Smiley, Robert F.; and Horne, Walter B.: Mechanical Properties of Pneumatic Tires with Special Reference to Modern Aircraft Tires. NASA TR R-64, 1960.

REPRODUCIBILITY OF THE
ORIGINAL PAGE IS POOR



(a) Tire profile.



(b) Tire footprint under a vertical
load of 56.1 kN (12 620 lb).



(c) Tire footprint under a vertical
load of 69.1 kN (15 530 lb).

Figure 1.- Profile and footprints of 30 x 11.5-14.5 tire used in investigation.
Tire inflation pressure = 1827 kPa (265 psi).

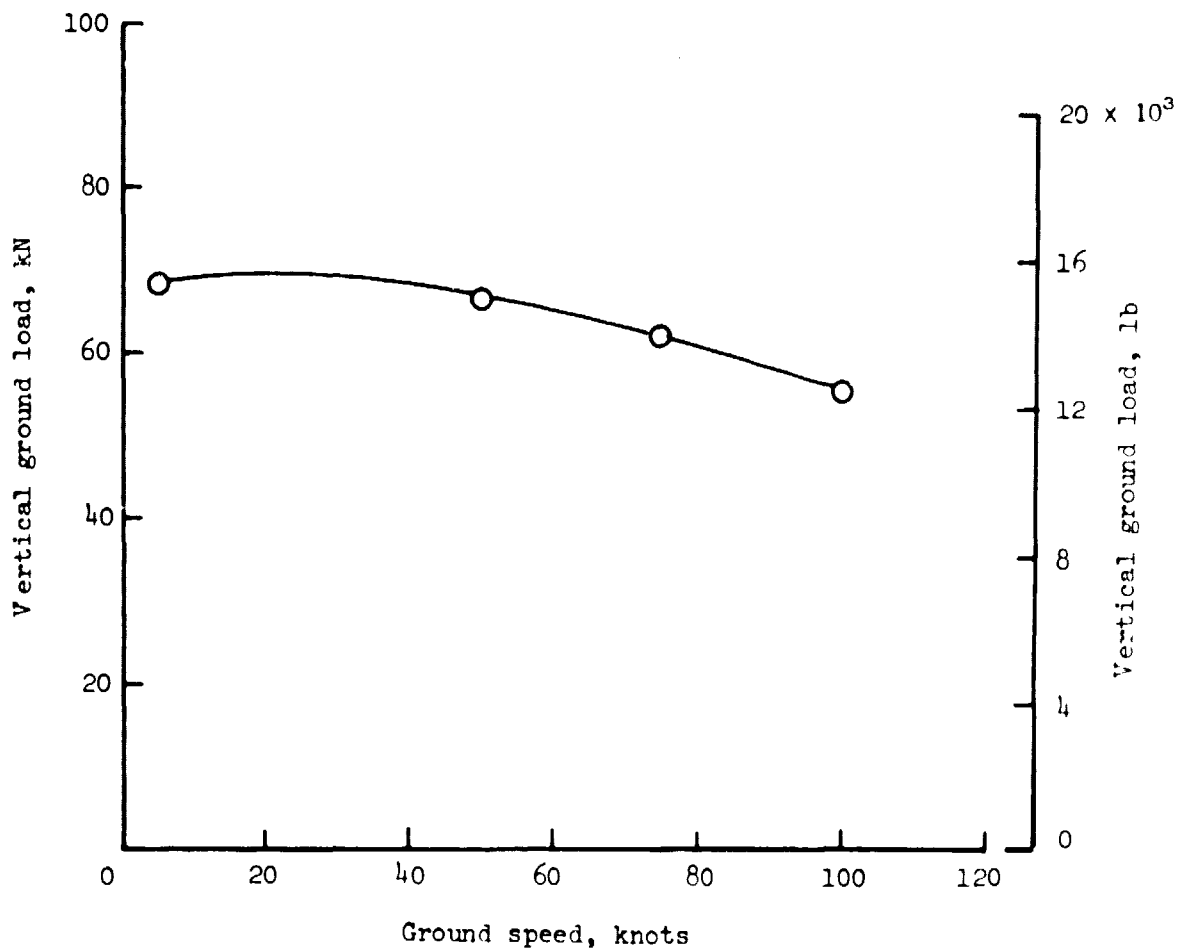
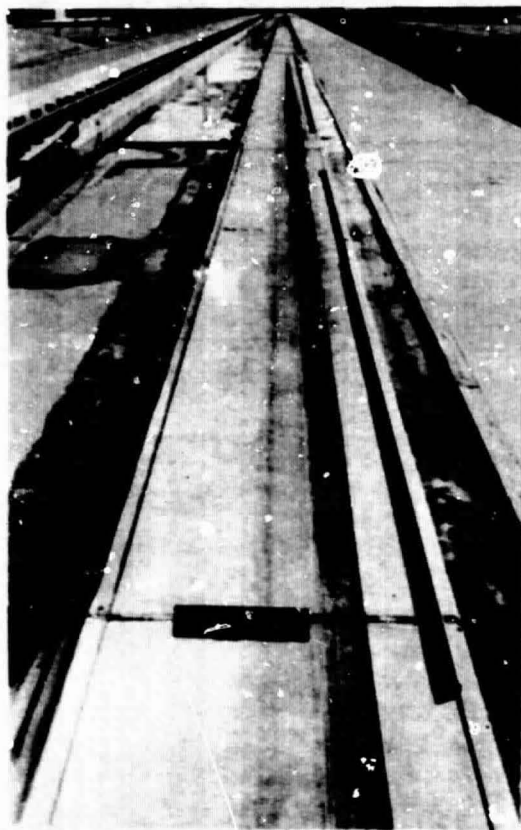


Figure 2.- Variation of tire vertical ground load with ground speed.
(Unpublished data obtained from flight tests.)

Dry



Wet



Flooded



Figure 3.- Photograph of dry, wet, and flooded test surfaces used in investigation.

REPRODUCTION OF THIS
ORIGINAL PAGE IS POOR

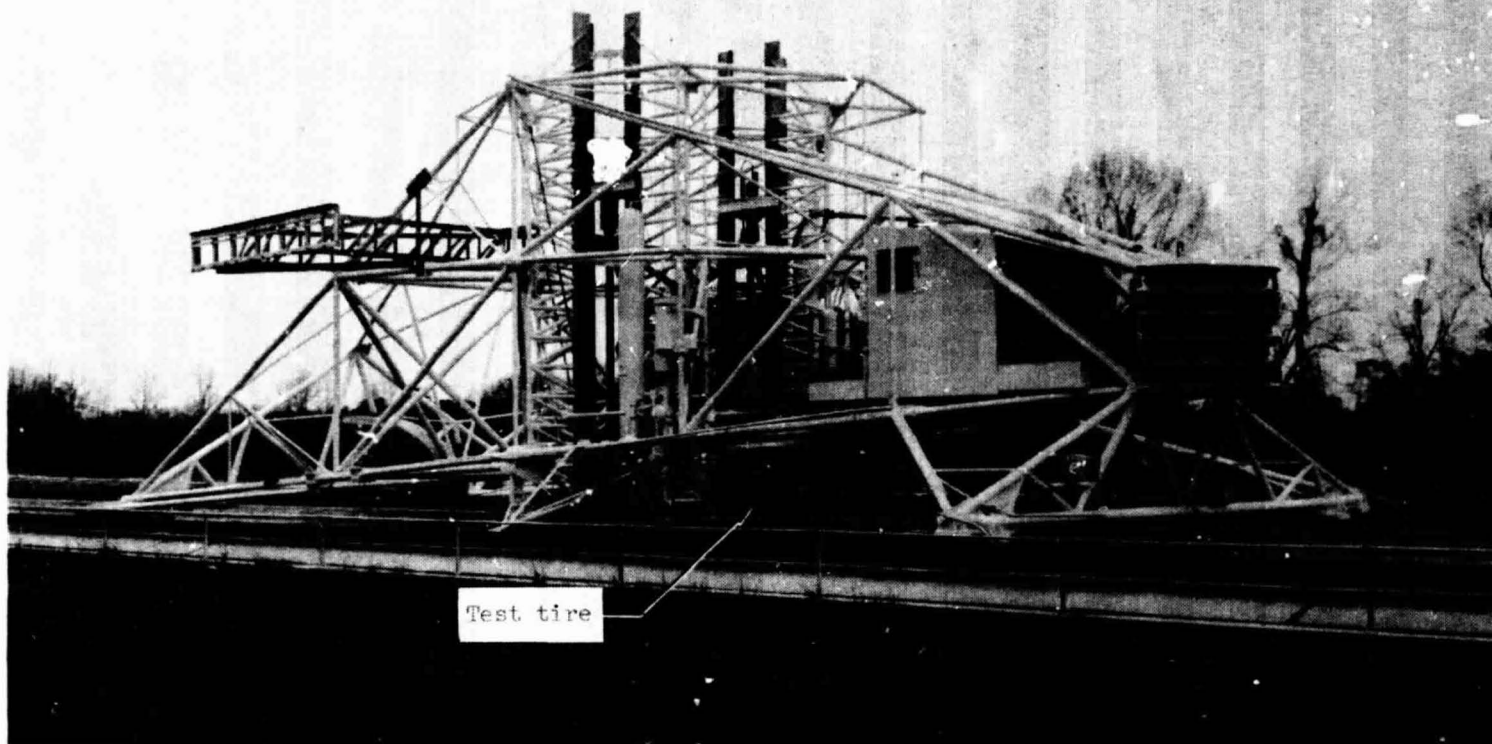


Figure 4.- Main test carriage at the Langley aircraft landing loads and traction facility.

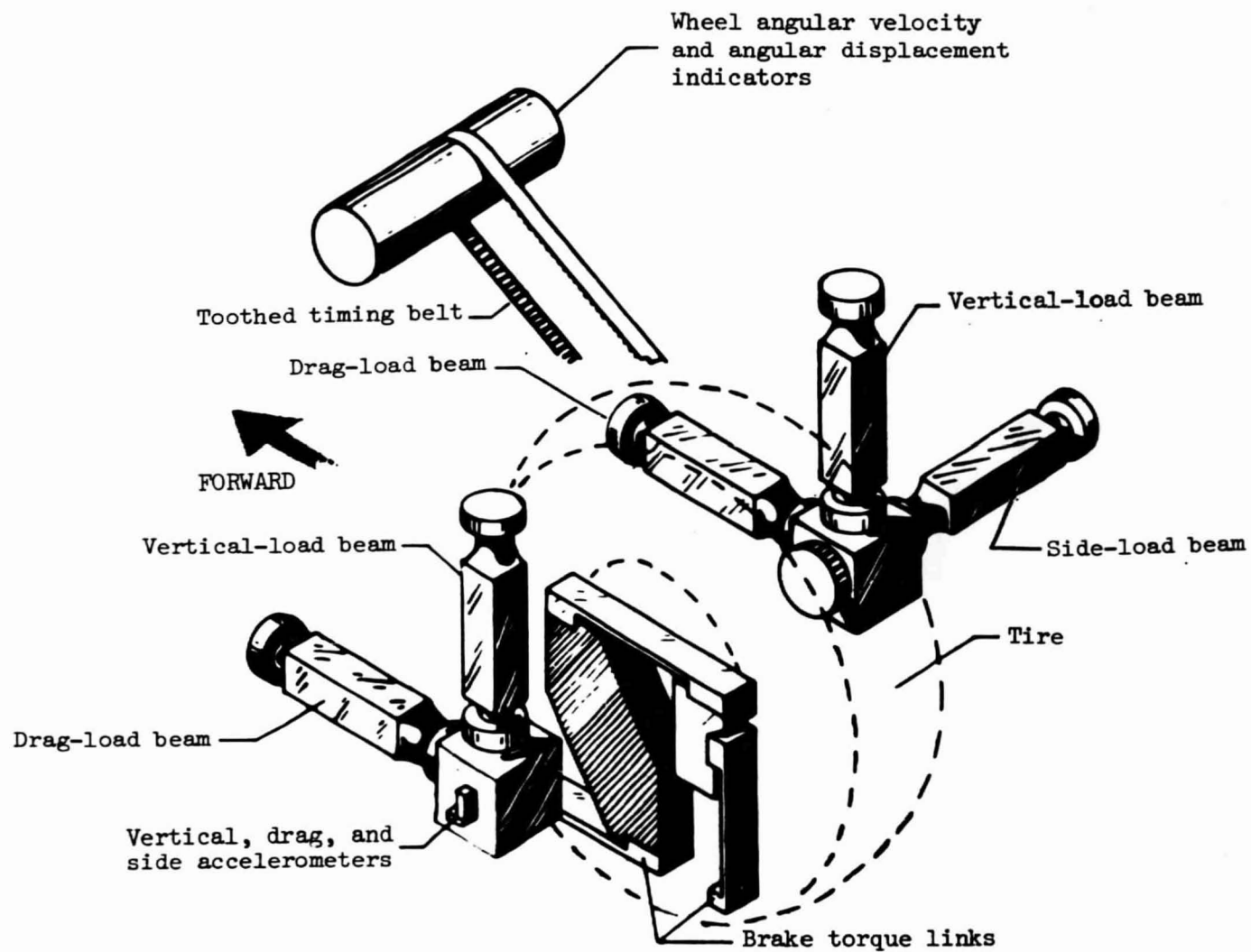


Figure 5.- Schematic of dynamometer used in tests.

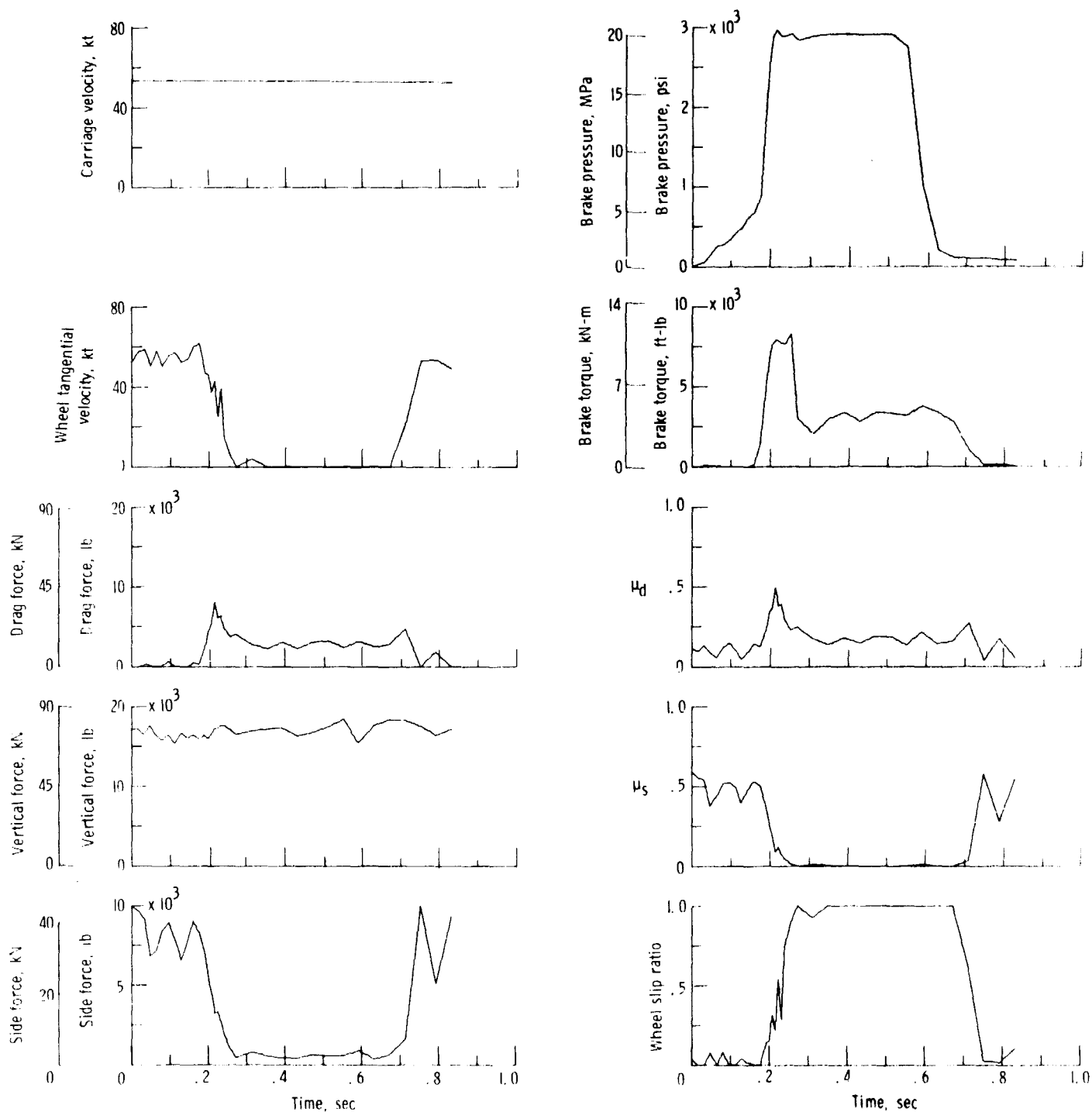


Figure 6. - Typical time histories of various parameters recorded and computed for test run brake cycles.
Yaw angle = 12°; ground speed = 51 knots; dry concrete surface.

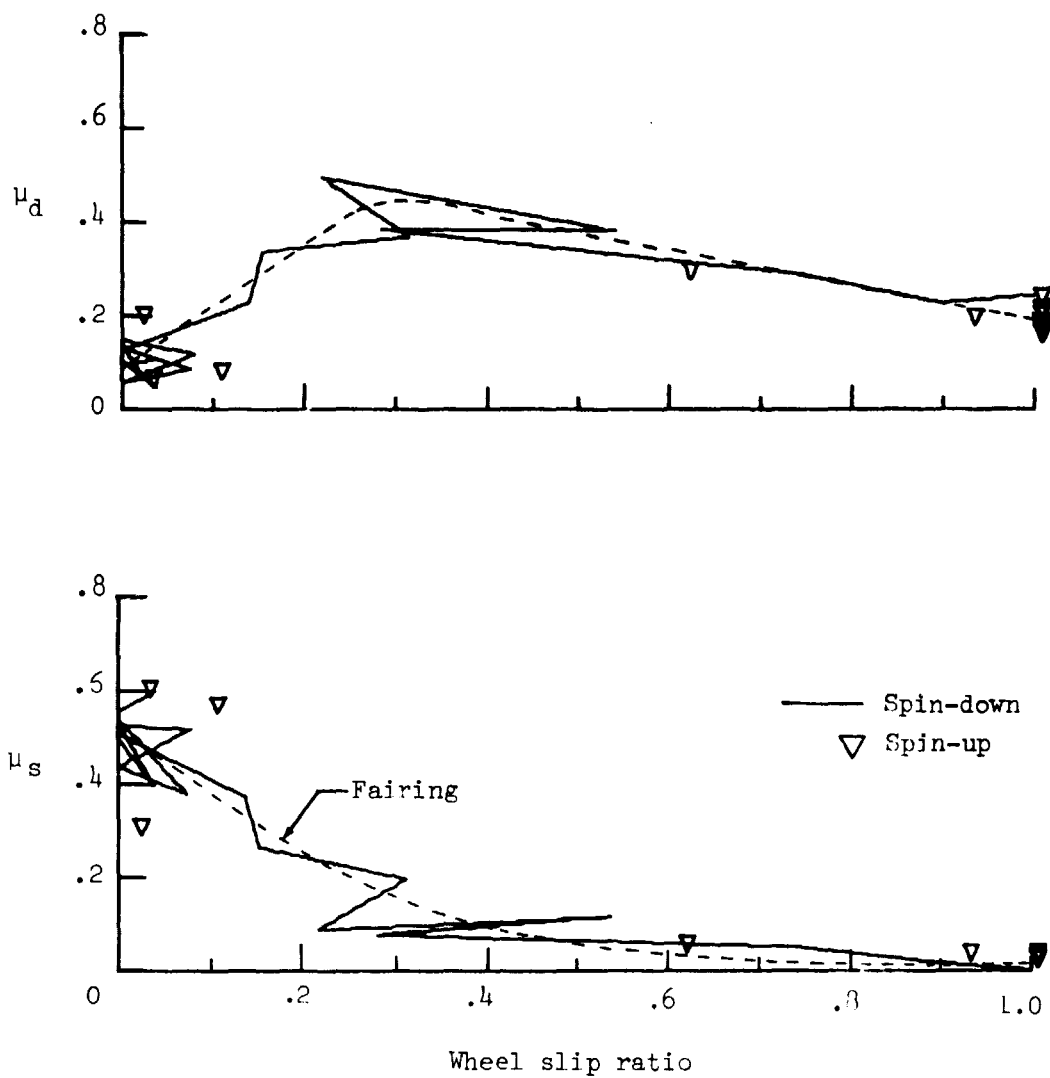
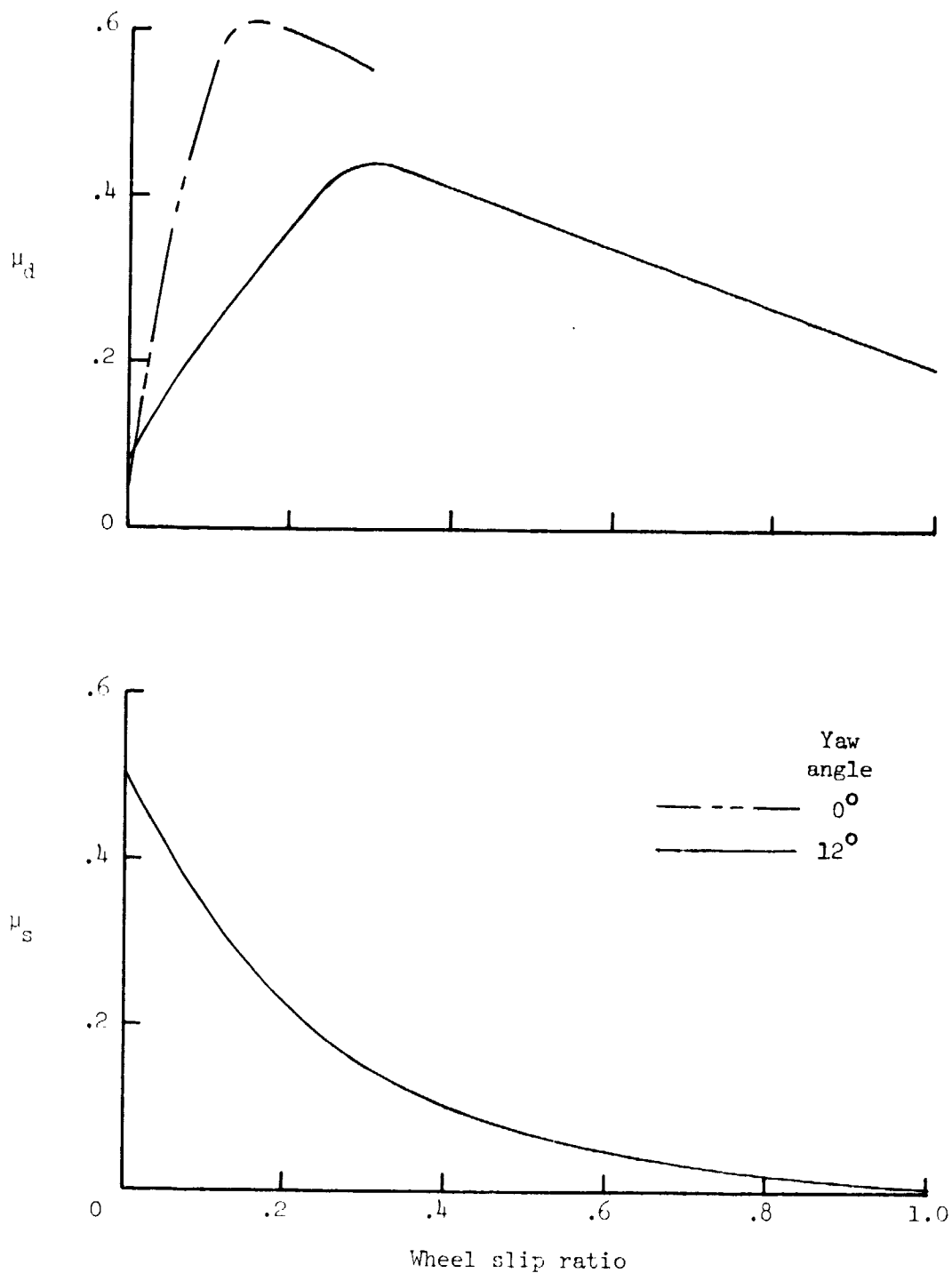
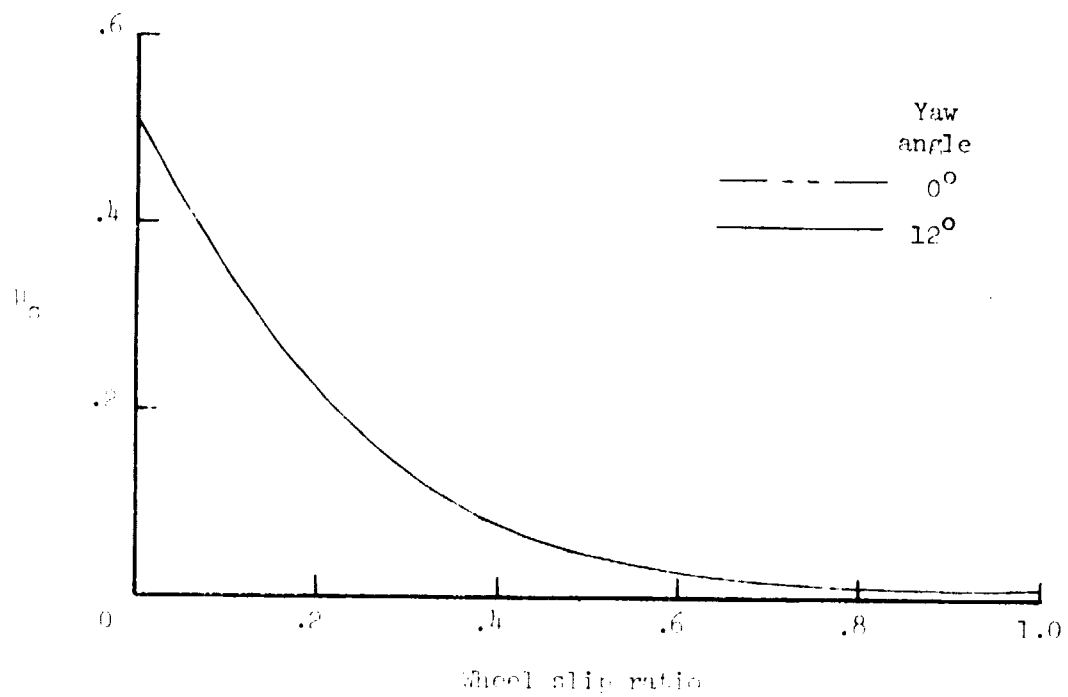
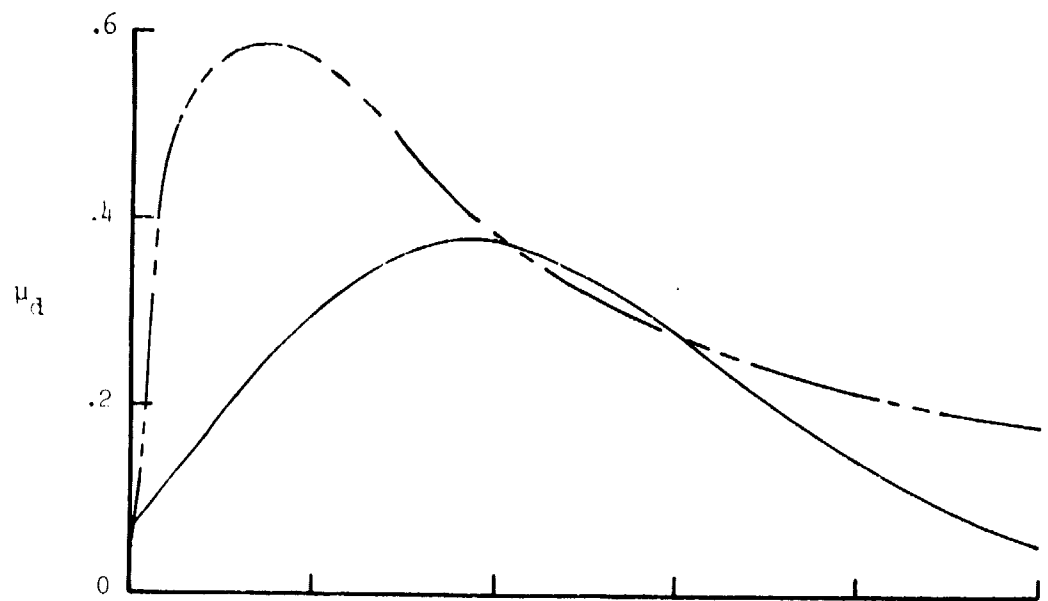


Figure 7.- Variation of computed friction coefficients with wheel slip ratio during a brake cycle on dry concrete surface.



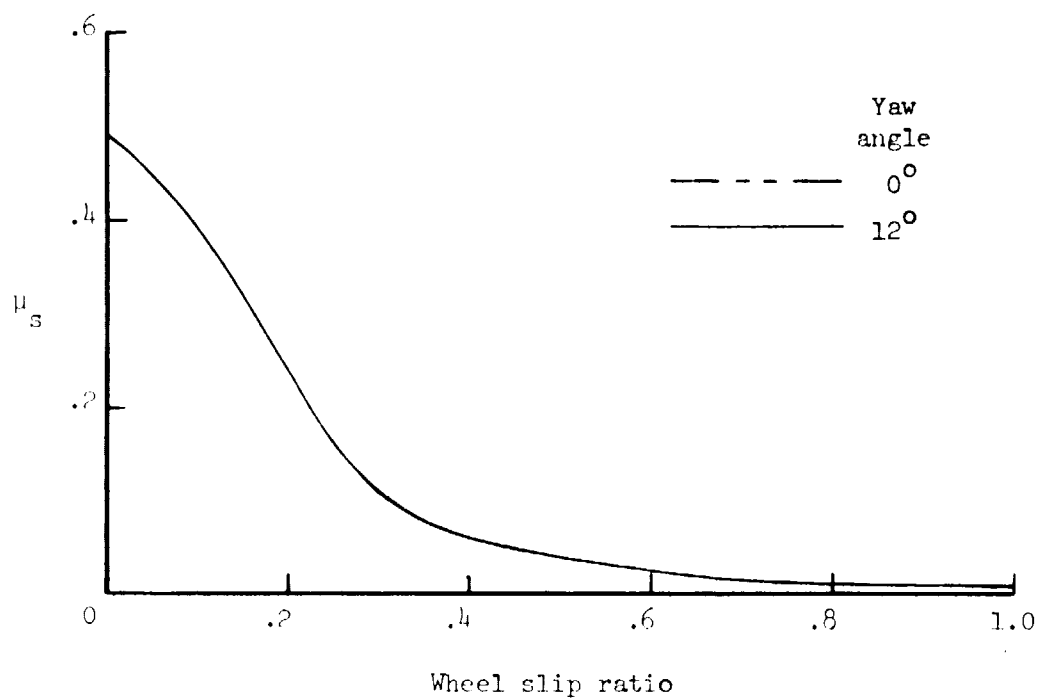
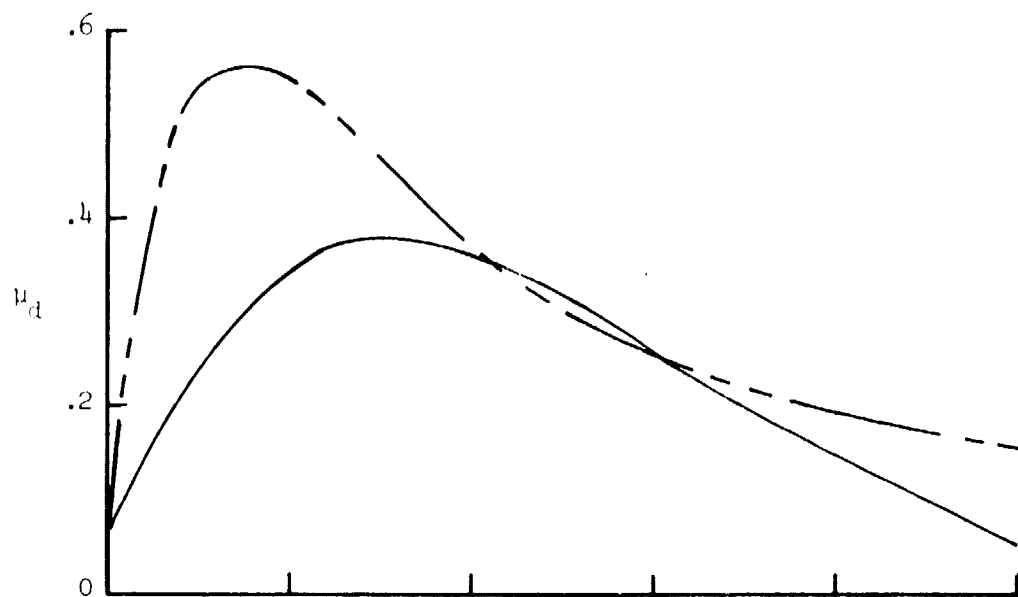
(a) Ground speed \approx 50 knots

Figure 8.- Variation of drag-force friction coefficient μ_d and cornering-force friction coefficient μ_s with wheel slip ratio for test tire at various ground speeds and yaw angles on a dry concrete surface.



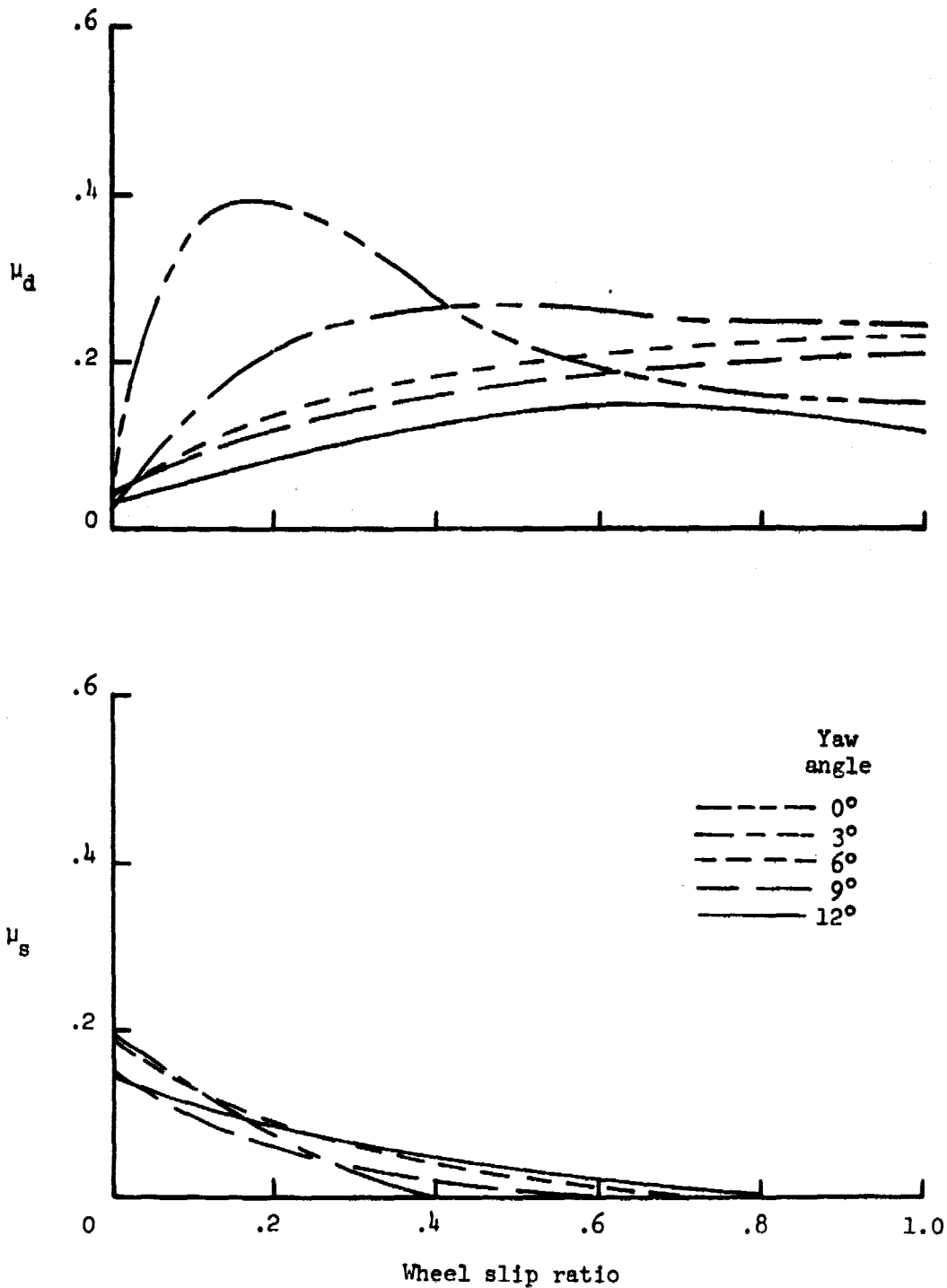
(b) Ground speed \approx 75 knots.

Figure 8.- Continued.



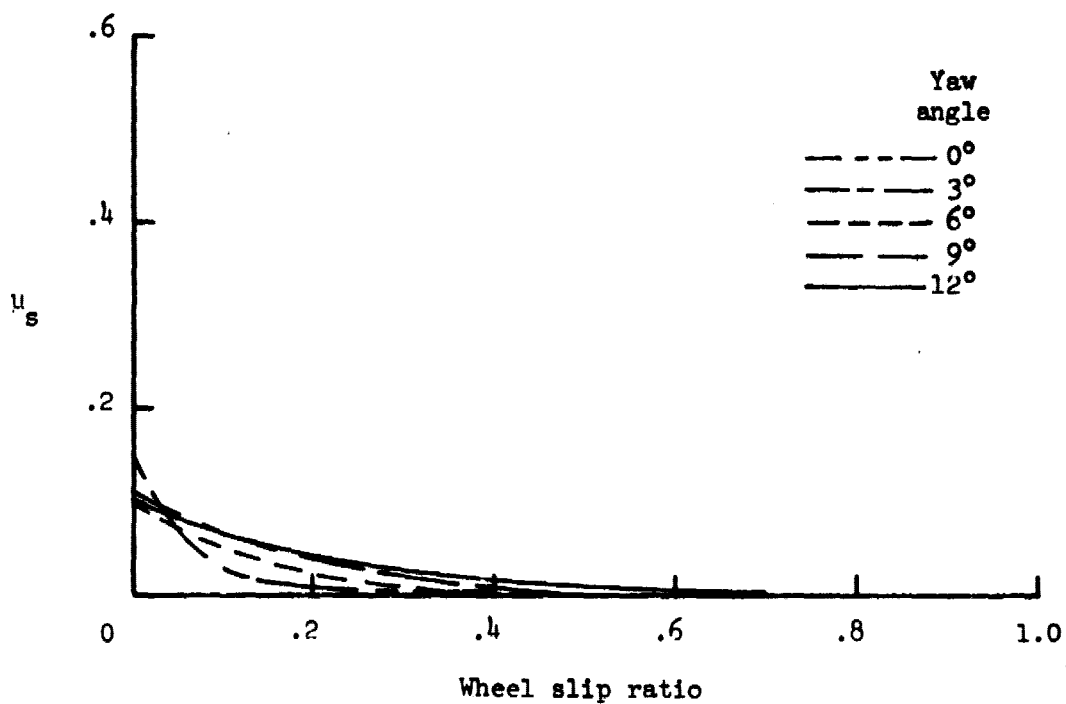
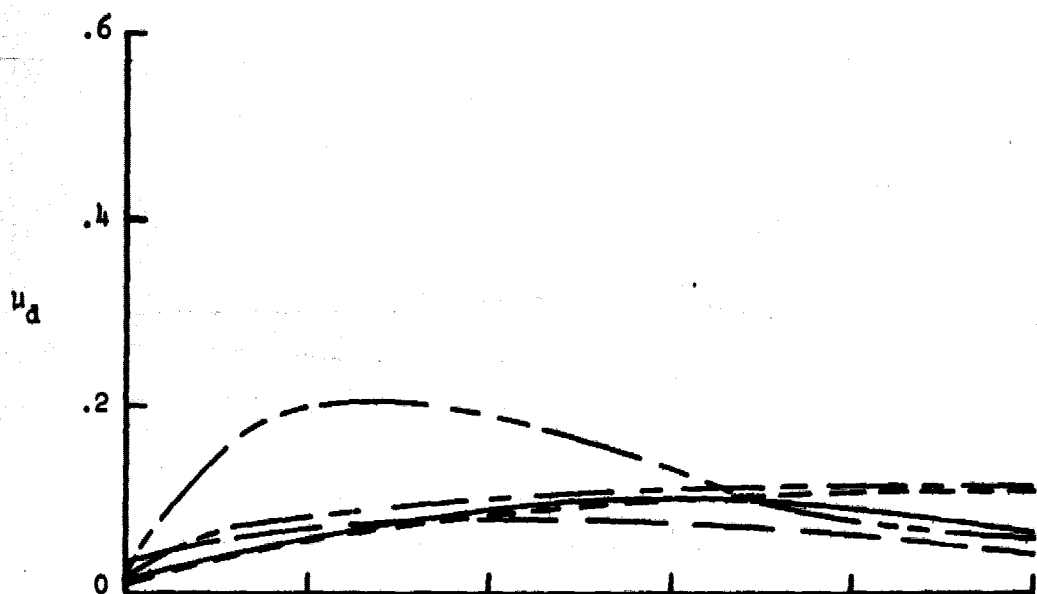
(c) Ground speed \approx 100 knots.

Figure 8.- Concluded.



(a) Ground speed \approx 50 knots.

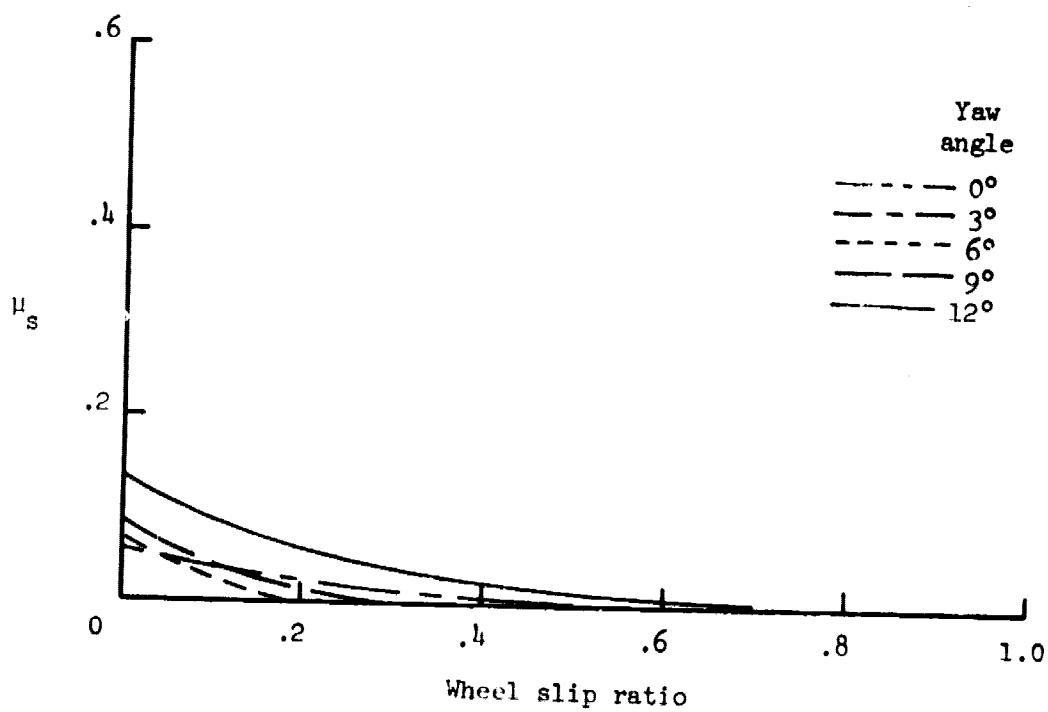
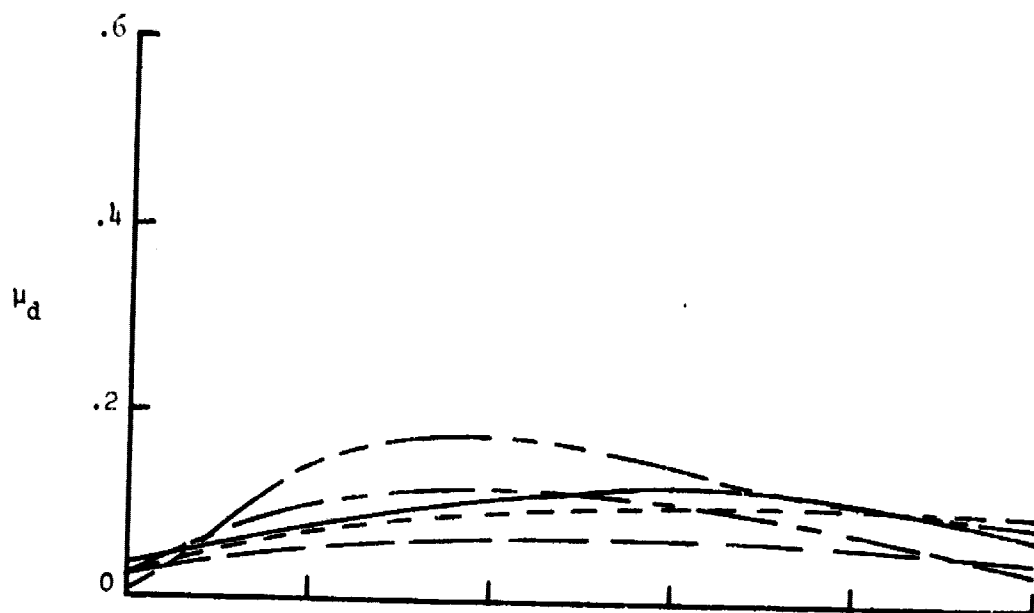
Figure 9.- Variation of drag-force friction coefficient μ_d and cornering-force friction coefficient μ_s with wheel slip ratio for test tire at various ground speeds and yaw angles on a wet concrete surface. Average water depth = 0.0.5 to 0.08 cm (0.02 to 0.03 in.).



(b) Ground speed \approx 75 knots.

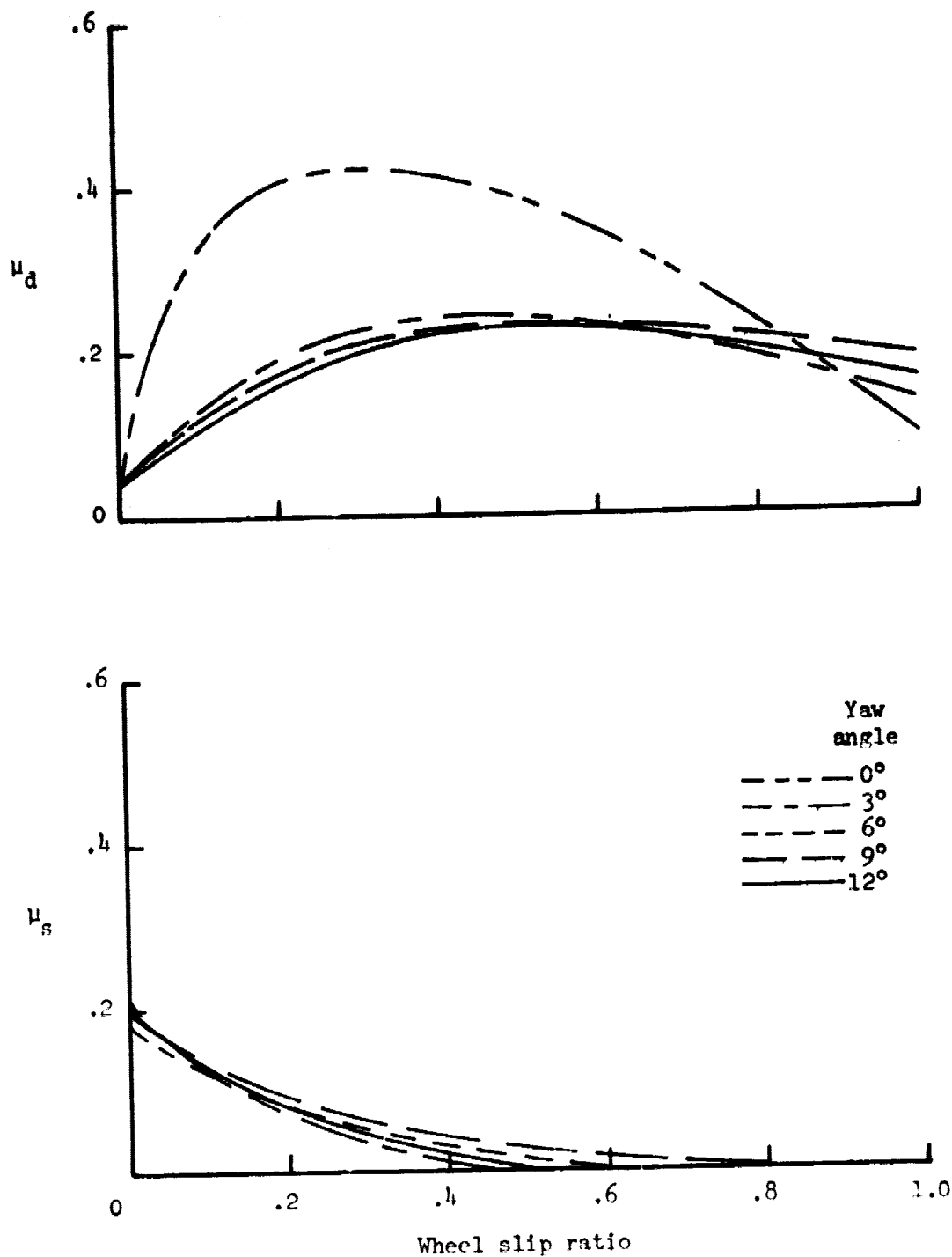
Figure 9.- Continued.

REPRODUCIBILITY OF THE
ORIGINAL PAGE IS POOR



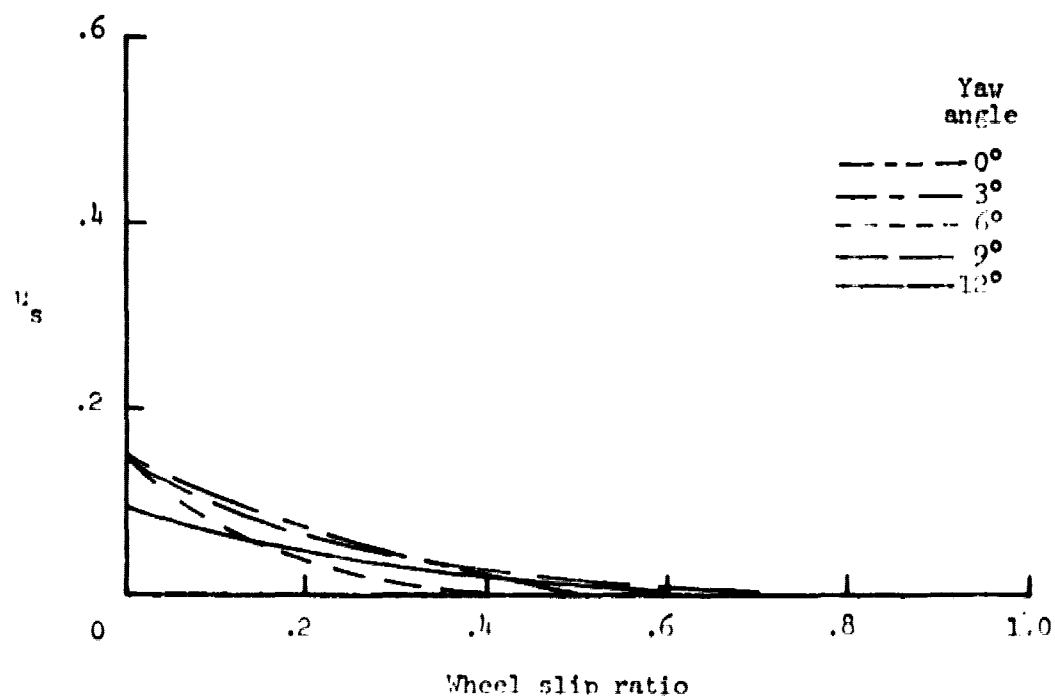
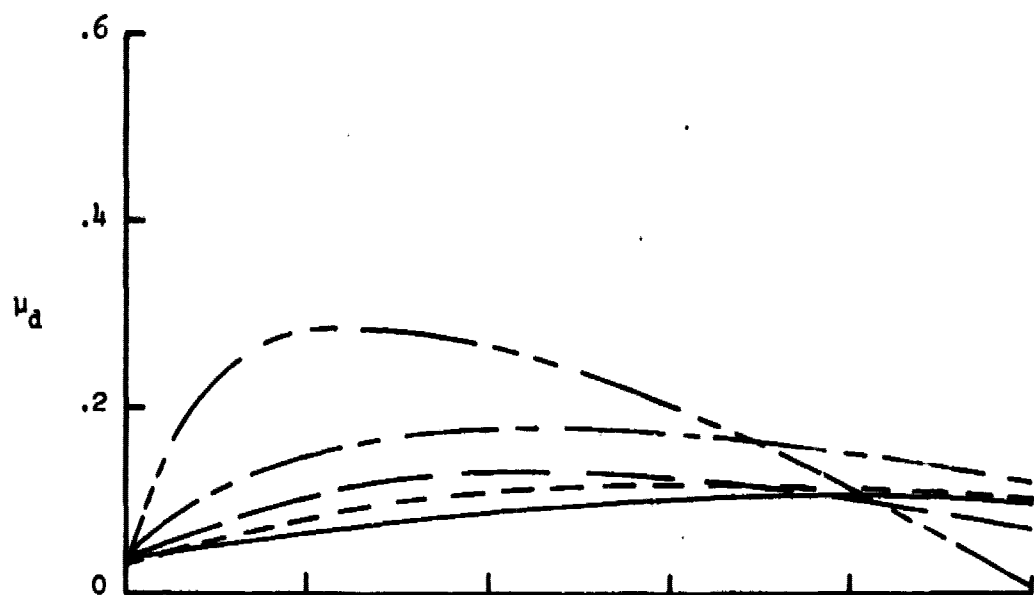
(c) Ground speed \approx 100 knots.

Figure 9.- Concluded.



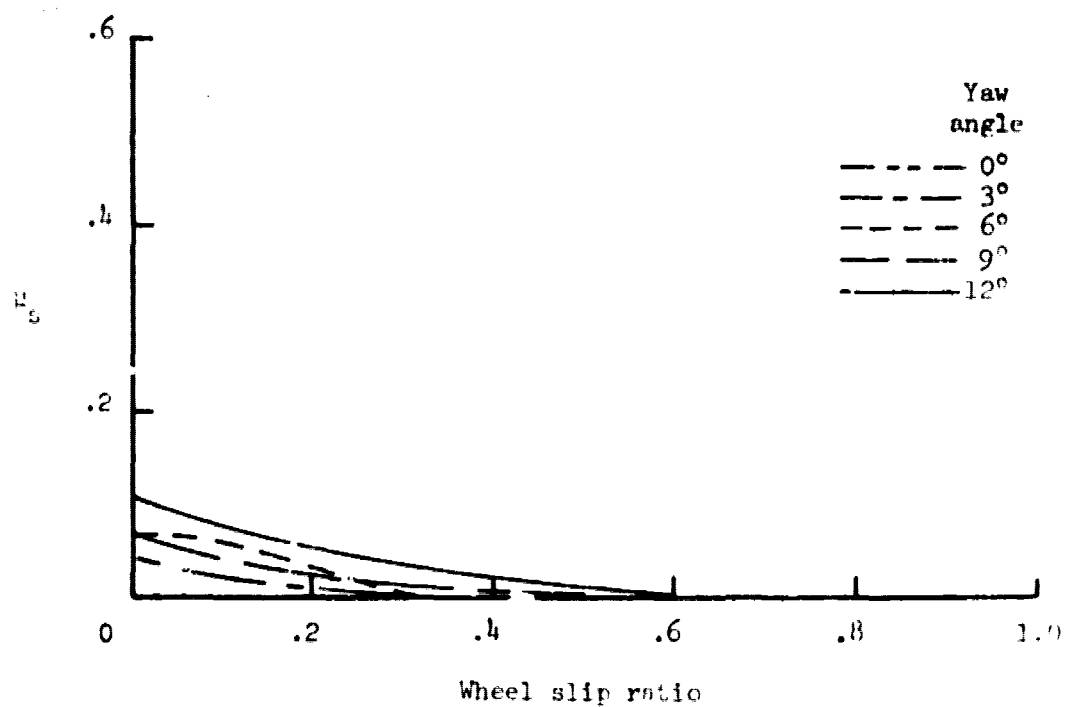
(a) Ground speed \approx 50 knots.

Figure 10.- Variation of drag-force friction coefficient μ_d and cornering-force friction coefficient μ_s with wheel slip ratio for test tire at various ground speeds and yaw angles on a flooded concrete surface. Average water depth = 0.5 to 0.8 cm (0.2 to 0.3 in.).



(b) Ground speed \approx 75 knots.

Figure 10.- Continued.



(c) Ground speed \approx 100 knots.

Figure 10.- Concluded.

REPRODUCED FROM THE
ORIGINAL

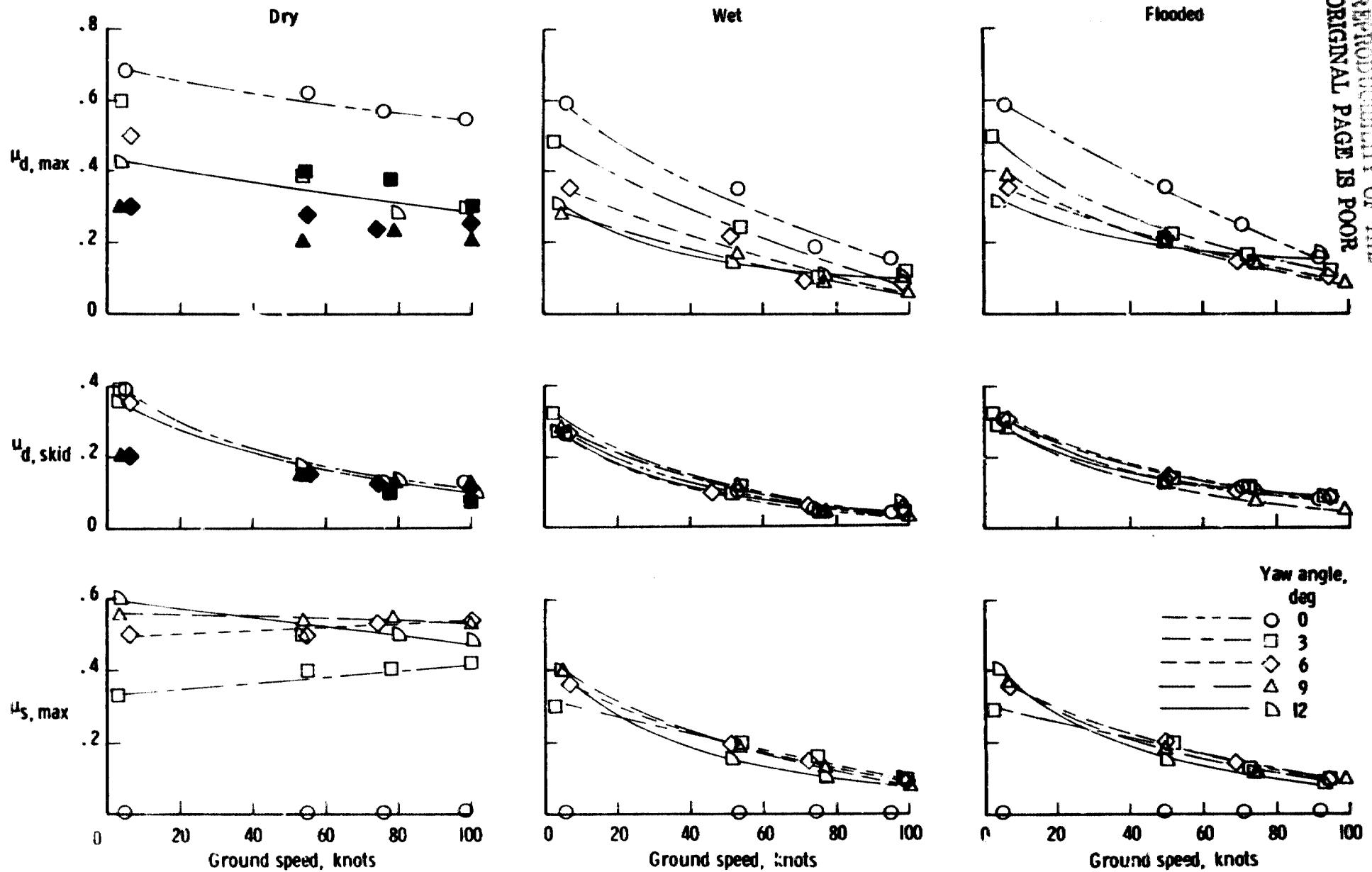


Figure 11. - Variation of maximum drag-force friction coefficient $\mu_{d, \max}$, skidding drag-force friction coefficient $\mu_{d, \text{skid}}$, and maximum cornering-force friction coefficient $\mu_{s, \max}$ with ground speed at various yaw angles on dry, wet, and flooded surfaces. (Closed symbols denote rubber contaminated surface)

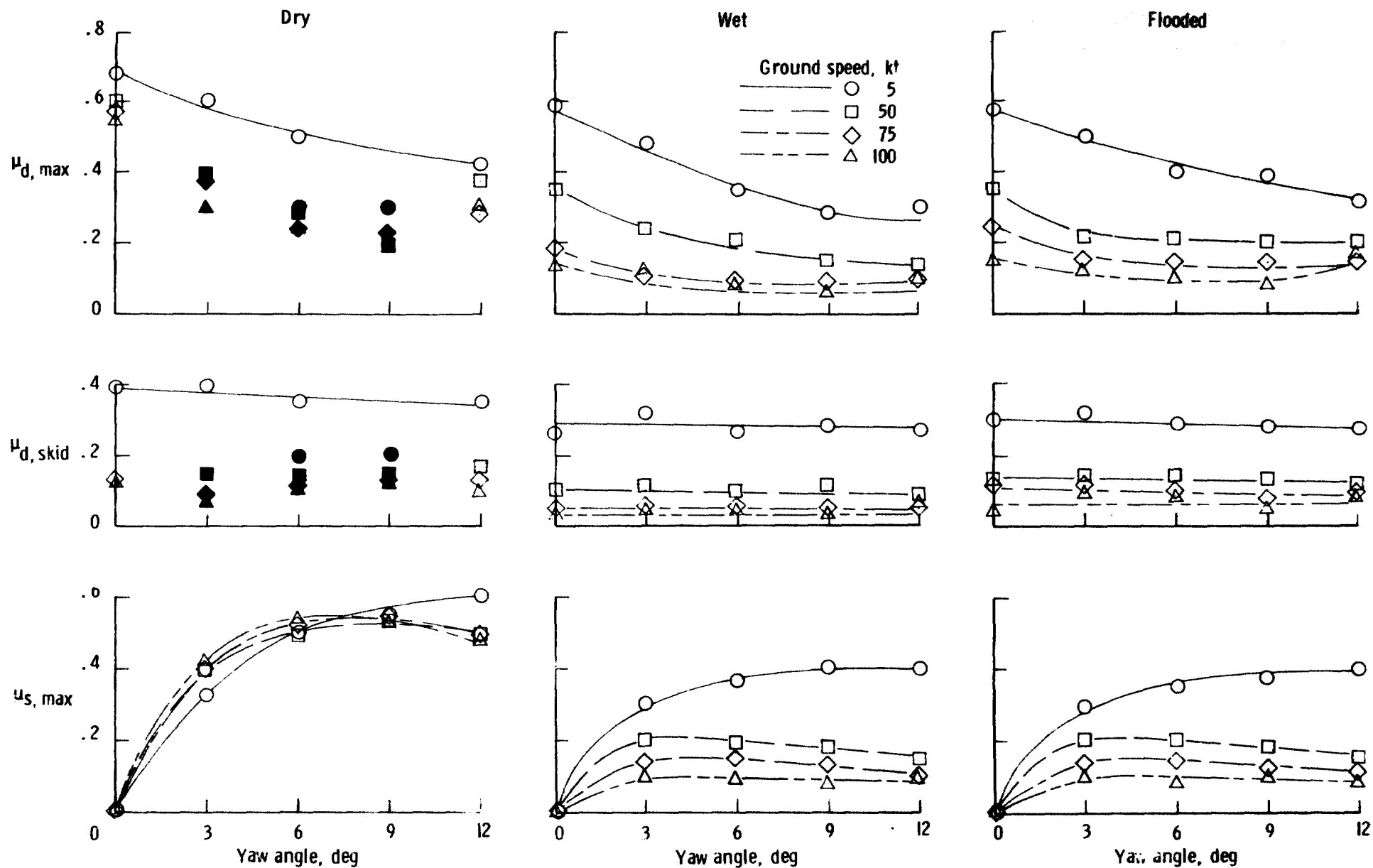


Figure 12. - Effect of yaw angle on maximum drag-force friction coefficient $\mu_{d, max}$, skidding drag-force coefficient $\mu_{d, skid}$, and maximum cornering-force friction coefficient $\mu_{s, max}$ at various ground speeds on dry, wet, and flooded surfaces. (Closed symbols denote rubber contaminated surface.)